Journal of Inorganic Biochemistry 275 (2026) 113138

Contents lists available at ScienceDirect

Journal of Inorganic Biochemistry

journal homepage: www.elsevier.com/locate/jinorgbio

Copper(II) and zinc(II) complexes of dimeric 8-hydroxyquinoline ligands: Synthesis, metal speciation, and biological evaluation

Roberta Panebianco [a], Giuseppina D.G. Santonoceta [a], Roberta Borrelli [a], Maria G.G. Pittalà [a], Rosaria Saletti [a], Carmelo Sgarlata [a], Maurizio Viale [b], Salvatore Furnari [c], Virginia Fuochi [c], Pio M. Furneri [c], Tommaso Mecca [d], Graziella Vecchio [a,*]

[a] Dipartimento di Scienze Chimiche, Università degli Studi di Catania, Viale A. Doria 6, 95125 Catania, Italy
[b] IRCCS Ospedale Policlinico San Martino, U.O. Bioterapie, L.go R. Benzi, 10, 16139 Genova, Italy
[c] Department of Biomedical and Biotechnological Sciences, Università degli Studi di Catania, via Santa Sofia 97, Catania 95124, Italy
[d] Institute of Biomolecular Chemistry CNR-ICB, Via Paolo Gaifami 18, Catania, Italy

ARTICLE INFO

Keywords:
Antimicrobial
Cancer
Chelator
Copper
Quinoline
Zinc

ABSTRACT

Hydroxyquinolines have garnered considerable attention due to their biomedical potential, particularly their ability to coordinate metal ions, which significantly influences their biological activity.

In this study, a series of 8-hydroxyquinoline dimeric derivatives was synthesized and compared to their monomeric counterparts. The metal-binding properties of these compounds with zinc(II) and copper(II) ions were investigated using ESI-MS spectrometry and UV–Vis spectrophotometry. The results revealed that 8-hydroxyquinoline dimers form highly stable metal complexes.

Biological studies have demonstrated that the functionalization of the 8-hydroxyquinoline scaffold modulates its activity: the introduction of amine chains in monomeric systems decreases the antiproliferative effects, both in the ligands and their metal complexes. Notably, the dimer derivative linked *via* diaminoethane exhibited the most potent antiproliferative and antibacterial activities. In contrast, the introduction of a diaminodioxaoctane linker reduced toxicity in bacteria and cancer cells, highlighting its promise as a biologically compatible metal-chelating agent.

1. Introduction

Metal chelators play an important role in medicinal chemistry [1], regulating metal homeostasis [2], detoxifying harmful metals [3], and serving as diagnostic [4] or therapeutic agents [5–7].

Chelators can inhibit metalloenzymes [8] or modulate oxidative stress [9] with a variety of applications, such as coadjuvants in antibiotic therapy [10–12] or in chemotherapy [6,13]. Some common chelators used in clinical settings are EDTA, deferoxamine, deferiprone, penicillamine and poliazamacrocycles [1]. Other chelators and their metal complexes have been widely studied, including terpyridines [14] and salens [15,16]. The design of new chelating agents is crucial for developing systems with high stability, biocompatibility and selectivity.

8-Hydroxyquinolines (8-HQs) represent a class of chelators that have received significant attention in the field of medicinal and inorganic chemistry [17–20]. The 8-HQ scaffold is a well-established pharmacophore that has been widely explored for its broad-spectrum biological activities, including antibacterial, antifungal, antiviral, and anticancer effects, as well as for the development of potent drug candidates [19–23]. The stability constants of 8-HQ with a range of metal ions have

Abbreviations: **8-HQ**, 8-Hydroxyquinoline; **Boc-en**, Boc-ethylenediamine; **CFU**, Colony-Forming Unit; **CQ**, 5-chloro-7-iodo-8-hydroxyquinoline, Clioquinol; **DMEM**, Dulbecco's Modified Eagle Medium; **EDTA**, Ethylenediaminetetraacetic acid; **En**, Ethylenediamine; **Etox**, 1,2-Bis(2-aminoethoxy)ethane; **FBS**, Fetal bovine serum; **HQ_2en**, 2,2′-((ethane-1,2-diylbis(azanediyl))bis(methylene))bis(quinolin-8-ol); **HQ_2etox**, 2-(((2-(2-(2-aminoethoxy)ethoxy)ethyl)amino) methyl)quinolin-8-ol; **HQCA**, 8-Hydroxyquinoline-2-carboxaldehyde; **HQen**, 2-(((2-aminoethyl)amino)methyl)quinolin-8-ol; **HQetox**, 2,2′-(5,8-dioxa-2,11-diazadodecane-1,12-diyl)bis (quinolin-8-ol); **MH**, Mueller-Hinton; **MOPS**, 3-morpholinopropane-1-sulfonic acid; **PBT2**, 2-(dimethylamino)methyl-5,7-dichloro-8-hydroxyquinoline; **ROS**, Reactive oxygen species; **RPMI**, Roswell Park Memorial Institute Medium; **SMON**, Subacute myelo-optic neuropathy; **TMS**, Tetramethylsilane; **TPEN**, N,N,N′,N′-tetrakis(2-pyridylmethyl)ethylenediamine.

* Corresponding author.
E-mail address: gr.vecchio@unict.it (G. Vecchio).

https://doi.org/10.1016/j.jinorgbio.2025.113138
Received 5 September 2025; Received in revised form 31 October 2025; Accepted 3 November 2025
Available online 4 November 2025

been determined [24,25], with copper(II) showing log β_1 and log β_2 values of 12.0 and 22.9, respectively, while with zinc(II) logβ_1 is 8.52 and log β_2 is 15.8 [24,26].

Clioquinol (5-chloro-7-iodo-8-hydroxyquinoline, CQ) is one of the most famous 8-HQ derivatives due to its clinical history [27]. During the 1950s, it was commonly used as an antibiotic for managing diarrheal diseases and dermal infections [28]. A significant number of cases of a severe and irreversible syndrome called subacute myelo-optic neuropathy (SMON) were correlated with the overuse of CQ. It has been suggested that the CQ ability to chelate copper induced SMON [29]. After this epidemiological study, the oral administration of CQ was banned [28]. In the 2000s, CQ attracted renewed scientific interest and became a prototype of metal-protein attenuating compounds [30]. Successive investigations have shown interest in CQ and its successor PBT2 (2-(dimethylamino)methyl-5,7-dichloro-8-hydroxyquinoline) as potential modulators of metal homeostasis in the context of neurodegenerative diseases such as Alzheimer's and Huntington's disease [7].

Numerous biological activities of 8-HQs have been associated with their ability to form biometal-based complexes [31,32]. Furthermore, complexes with non-biological metals have been investigated for their biological activities [33–35].

Among the various reported biological activities of 8-HQ derivatives, their anticancer properties both *in vitro* and *in vivo* preclinical models are particularly noteworthy, given the ongoing need for novel anticancer compounds [17–19,36–38].

CQ exhibits anticancer properties [14,16,26,27] and has been studied in clinical trials in patients with leukemia, myelodysplasia, non-Hodgkin lymphoma, Hodgkin's lymphoma, and multiple myeloma [27]. It has been documented that the interaction with copper(II) ions is essential for the manifestation of anticancer activity in both CQ and other 8-HQs [16,32–34]. Many hypotheses have been proposed to explain the toxicity. Some 8-HQs act as ionophores, transporting metal ions (Cu and Zn) across cellular membranes. This dyshomeostasis of the metals in cells leads to increased production of reactive oxygen species (ROS) and copper complexes of HQs can inhibit proteasome activity [16].

Various HQ derivatives have been synthesized over the years, incorporating different moieties and exhibiting new properties [18,21,39–42]. Furthermore, several bis-8-HQ derivatives with few atom linkers have been designed to exploit their complexation ability and chelate the metal ion with the two HQ rings in a coordination environment similar to HQ in $M(HQ)_2$ species [43].

Dimers inhibited the precipitation of Aβ-peptides induced by Cu^{2+} and Zn^{2+} more efficiently than the corresponding monomers and have been proposed as potential anti-Alzheimer's agents [43–46]. Nevertheless, limited data are available for dimeric systems on the most investigated biological properties of HQs, such as anticancer and antibacterial activities [47]. For this reason, we synthesized new 8-HQ dimeric derivatives (Fig. 1) and their monomeric analogs with longer linkers to study their coordination behavior with copper(II) and zinc(II).

We determined the conditional stability constants of the complexes and the speciation using UV–Vis spectroscopy. Complex species were characterized by ESI-MS. Speciation is particularly relevant for biological applications since specific biological activity can be attributed to the presence of a given complex species. We also evaluated the antiproliferative activity of the ligands alone and in the presence of zinc(II) and copper(II) against A2780 and MDA-MB-231 cancer cell lines, as well as their antibacterial efficacy against both Gram-positive and Gram-negative bacteria.

2. Results and discussion

2.1. Synthesis and characterization of the ligands

The ligands were designed to have additional donor atoms in the chains based on the hypothesis that this feature would improve the stability of the metal complexes compared to 8-HQ. HQen and HQetox have, respectively, an diaminoethane and a diaminodioxaoctane chain, while HQ_2en and HQ_2etox have two hydroxyquinoline rings and a linker containing two nitrogen atoms.

New 8-HQ derivatives with two 8-HQ moieties and their corresponding mono-derivatives (Fig. 1) were synthesized by reductive amination from 8-hydroxyquinoline-2-aldehyde and the amine linker as reported in the synthesis scheme (Fig. S1). They were purified by flash chromatography using a C18 reversed-phase column. The ligands were all obtained in good yields (30 %–70 %) and high purity. They were characterized by ^{1}H and ^{13}C NMR, UV–Vis spectroscopy and ESI-HRMS spectrometry (Figs. S2-S6). ESI-HRMS data compared with the calculated mass values are reported in Table S1, and the spectra of the monocharged molecular ions of synthesized ligands are shown in Figs. S3-S6. The ligand-Na^+ adducts are also present in all the spectra.

^{1}H and ^{13}C NMR spectra confirmed the formation of the products. In all the spectra, the signals due to the hydroxyquinoline ring are evident, together with the signals of the amino chain. In the ^{1}H NMR spectra of dimers, the quinoline rings were equivalent and the spectra in the aliphatic region were simplified due to the symmetry of the molecule. All the methylene groups resonate as singlets (Fig. S2).

In the UV–Vis spectra of the ligands, typical bands of the 8-HQ chromophore at 242 nm and 310 nm can be assigned to π-π* and n-π* transitions [48]. The spectra depend on the pH due to the deprotonation of the phenolic group. The band at 242 nm reduced as the pH increased, and a new band appeared at 258 nm. A similar trend was observed for the band at 310 nm, which shifted to 350 nm. HQen was monitored in the pH range from 1.6 to 12.4. Spectra of HQen at different pH values are reported in Fig. S7. Similar results were obtained for the other derivatives.

2.2. Metal complexes

2.2.1. UV–Vis spectroscopy and stability constants of Cu^{2+} and Zn^{2+} complexes

The metal complexes of the 8-HQ derivatives were investigated using

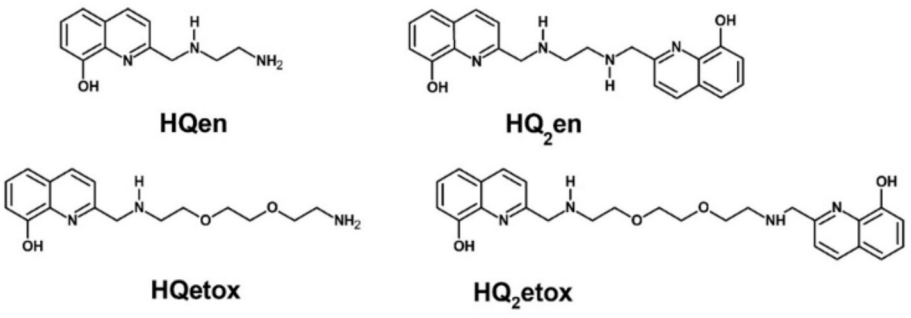

Fig. 1. 8-HQ derivatives included in this work.

UV–Vis spectroscopy in aqueous solution at pH 7.4 (MOPS buffer). The experimental conditions were chosen to simulate the physiological environment, while the use of MOPS as the buffer minimized/prevented metal ion complexation, an issue frequently encountered (but often overlooked) when more conventional buffering agents are employed [49].

The absorption bands in the spectra of HQen, HQ_2en, HQetox and HQ_2etox at ca 242 nm and 310 nm shifted upon adding Cu^{2+} or Zn^{2+} due to the deprotonation of the phenol group during the complexation (Figs. S8-S11) [48,50]. The UV–Vis spectra are similar to those reported for the copper(II) complex of 8-HQ and its derivatives [18,51–53].

As recommended for complexes with very high stability constants (log K > 6) [54], the formation of the metal complex species was assessed through competition spectrophotometric experiments using EDTA, which is commonly proposed as a convenient competitor for such strong ligands [46]. Titrations were typically conducted by incrementally adding the chelating agent to solutions containing the metal (M = Cu^{2+} or Zn^{2+}) and the ligand (L) in the proper stoichiometric ratio to examine the following overall equilibrium (charges are omitted for simplicity):

$$M_pL_q + pEDTA \rightleftarrows pM - EDTA + qL$$

In the case of HQ_2en, due to the markedly higher affinity of this bis-hydroxyquinoline ligand for both metal ions compared to EDTA, the ligand solution was titrated with the M-EDTA complex, allowing the investigation of the equilibrium below:

$$qL + pM - EDTA \rightleftarrows M_pL_q + pEDTA$$

A rigorous analysis of the complexation processes enabled overcoming the limitations typically associated with the spectrophotometric determination of very high binding constants that are often reported as "larger than a certain threshold value", which ultimately depends on the affinity of EDTA for a given metal ion. Representative UV–Vis competition experiments for HQ_2en with Cu^{2+} and Zn^{2+} are shown in Figs. 2 and 3, respectively. Competition titrations for the other ligands are in the Supporting Information (Figs. S12-S17).

A preliminary indication of the stoichiometry of the metal complex species was obtained from the molar ratio plots, which, in most cases, displayed two distinct inflection points upon the addition of 0.5 and 1 equivalents of EDTA to 1:1 or 2:1 metal-to-ligand (M/L) solutions (Figs. S12-S17). These features suggest the formation of multiple species in the solution, corresponding to ML and ML_2 complexes. The

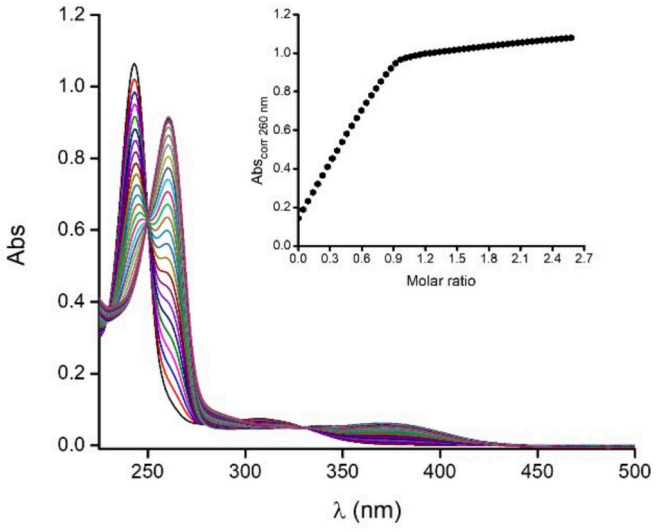

Fig. 2. UV–Vis titration of HQ_2en (1.81×10^{-5} M) with the Cu^{2+}-EDTA complex ($C_{EDTA} = 2.20 \times 10^{-4}$ M) at 25 °C and pH 7.4 (10 mM MOPS); inset: molar ratio plot.

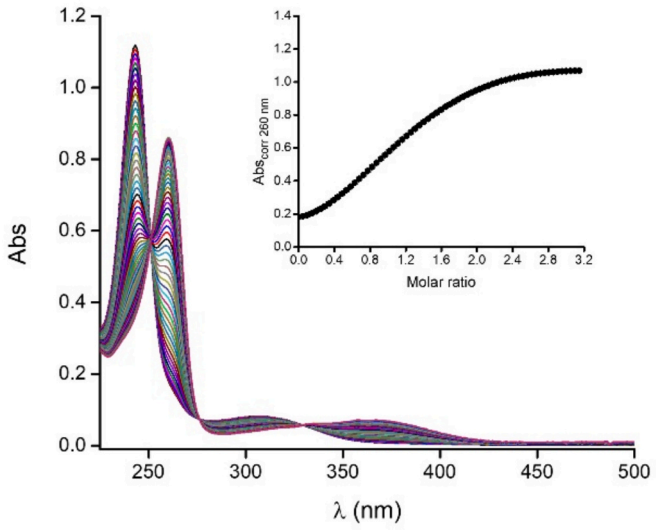

Fig. 3. UV–Vis titration of HQ_2en (1.81×10^{-5} M) with the Zn^{2+}-EDTA complex ($C_{EDTA} = 2.20 \times 10^{-4}$ M) at 25 °C and pH 7.4 (10 mM MOPS); inset: molar ratio plot.

stoichiometries of all the complex species, along with their conditional stability constants at pH 7.4, were determined through a multiwavelength analysis of the spectral data. Despite various speciation models and combinations of possible species being evaluated, the analysis consistently converged to the species listed in Table 1, which also includes the formation constants of the parent 8-HQ complexes calculated at the same pH conditions [26,55].

The HQen ligand forms two complex species, ML and ML_2, with both Cu^{2+} and Zn^{2+} ions (Figs. S18, S19). As expected, and observed for all ligands, the higher stability of the Cu^{2+} complexes compared to those of Zn^{2+} is in keeping with the Irving-Williams series and the values reported for other 8-HQ-based ligands [46,50]. The spectrophotometrically determined logK values for the ML species with both metal ions are larger than those calculated for the unsubstituted 8-HQ [56]. This suggests that the coordination of the metal with the nitrogen atom of the pyridine ring, the phenolate group and the amino groups of the side chain promotes the formation of five-membered chelate rings that enhance complex stability, as reported for other amino-8-hydroxyquinoline derivatives [50,57]. However, the additional nitrogen-coordinating atoms concurrently weaken the formation of the ML_2 complex, as evidenced by the lower $logK_2$ values compared to 8-

Table 1
Conditional stability constants for the formation of Cu^{2+} and Zn^{2+} complexes of HQen, HQ_2en, HQetox and HQ_2etox at 25 °C and pH 7.4 (MOPS 10 mM).

		Copper(II)		Zinc(II)	
Ligand	Species	logβ[a]	logK[a]	logβ[a]	logK[a]
HQen	*ML*	13.38 (3)	*13.38 (3)*	9.50 (1)	*9.50 (1)*
	ML_2	18.33 (2)	*4.95 (4)*[b]	15.24 (1)	*5.74 (2)*[b]
HQ_2en	*ML*	19.2 (1)	*19.2 (1)*	15.17 (1)	*15.17 (1)*
	ML_2	23.6 (4)	*4.4 (3)*[b]	20.03 (4)	*4.86 (4)*[b]
	M_2L	33.3 (2)	*14.1 (2)*[c]	29.88 (1)	*14.7 (1)*[c]
HQetox	*ML*	12.0 (1)	*12.0 (1)*	10.80 (5)	*10.80 (5)*
	ML_2	18.24 (2)	*6.24 (1)*[b]	16.01 (3)	*5.21 (6)*
HQ_2etox	ML	14.30 (5)	14.30 (5)	11.07 (6)	11.07 (6)
	ML_2	18.8 (1)	4.5 (1)[b]	16.30 (4)	5.22 (8)[b]
	M_2L	26.1 (2)	11.8 (2)[c]	20.8 (2)	9.7 (2)[c]
8-HQ[d]	ML	9.75	9.75	6.27	6.27
	ML_2	18.4	8.6[b]	11.3	5.0[b]

[a] Errors in the last significant digit are in parentheses.
[b] Refers to equilibrium ML + L ⇄ ML_2.
[c] Refers to equilibrium M + ML ⇄ M_2L.
[d] Calculated at pH 7.4 from ref.[26]

HQ. This can be attributed to the steric hindrance of the substituent at the 2-position of hydroxyquinoline that causes a reduced ability to accommodate a second ligand molecule within the metal coordination sphere [50,53].

The formation of ML and ML_2 complex species with Cu^{2+} and Zn^{2+} ions was also observed for the related dimeric HQ_2en ligand (Figs. S20, S21). Noticeably, this bis-hydroxyquinoline ligand exhibits a selectivity for Cu^{2+} over Zn^{2+} by 4 orders of magnitude in forming the ML species. Moreover, the presence of two hydroxyquinoline units allows the formation of an extra M_2L species. In general, complexes formed by HQ_2en exhibit remarkably high thermodynamic stability; the additional coordination unit in the molecular scaffold imparts an augmented complexing ability (5.7-–5.8 log units for both metal ions, when compared to the ML complex formed by HQen) than the simple hydroxyquinoline structure. This significant increase may be attributed to the chelation of the metal by two 8-HQ units, which, supported by the flexible and suitably sized bis-amino spacer, adopt an optimal concerted coordination geometry for an exceptionally stable mononuclear complex. We can hypothesize that the formation of the ML species involves the two 8-HQ moieties and the amino groups of the ethylene chain. The stability constant of ML species is significantly higher than that reported for similar ligands with a non-coordinating linker [43,44], in keeping with the involvement of the amino groups of the linker in the metal coordination.

For both metal ions, the stability of the M_2L species with L = HQ_2en, which refers to the coordination of a second metal ion at the additional hydroxyquinoline, is significantly higher than the value determined for the ML species formed by HQen. This evidence emphasizes the role of the bis-amino linker/double hydroxyquinoline arrangement in forming stable dinuclear complexes. As expected, the ML_2 species has conditional stability constants significantly lower than those calculated for 8-HQ.

The formation of ML and ML_2 complexes with both Cu^{2+} and Zn^{2+} ions also occurs with HQetox (Figs. S22, S23). The logK values determined for ML are larger than those calculated for 8-HQ, indicating the favorable contribution of the nitrogen atom in the chain, which increases the stability of the complex by fostering the formation of a chelating ring. Conversely, in particular for Cu^{2+}, the formation of ML_2 is disfavored when compared to the same complex with 8-HQ.

The corresponding HQ_2etox dimer forms very stable mono- and dinuclear Cu^{2+} and Zn^{2+} complexes along with ML_2 species (Figs. S24, S25). The logK value for the ML species with Cu^{2+} is 2.3 log units higher than that for the analogous monomer HQetox. The coordination of a second metal ion to the additional hydroxyquinoline unit and the formation of the M_2L species occur with a stability comparable to that observed for the formation of the ML complex by the monomeric HQetox. This suggests that the two 8-HQ moieties of the dimer HQ_2etox, due to the increased flexibility and extended length of the linker, act as nearly independent binding sites that may form dinuclear species with comparable stability as found for HQ_2en. Lastly, the ML_2 complexes exhibit reduced stability, in line with that observed for the other ligands studied [50].

While previous studies on dimeric 8-hydroxyquinoline ligands have primarily reported [43,44] the formation of highly stable 1:1 (ML) complexes with Cu^{2+} and Zn^{2+}, the HQ_2en and HQ_2etox dimers investigated in this work exhibit distinct coordination behavior, leading to the formation of species with variable metal-to-ligand stoichiometries. Moreover, HQ_2etox forms metal complexes with stability constants consistent with those reported for other 8-HQ-based dimers [44], while the complexes formed by HQ_2en are about four (Cu^{2+}) and two (Zn^{2+}) orders of magnitude more stable than those reported elsewhere [44], thus highlighting the enhanced chelating capacity of the newly proposed ligands. A proposed structure of the metal complexes is reported in Fig. S26.

2.3. Mass spectrometry

ESI-MS spectrometry data for the copper(II) and zinc(II) complexes of the new ligands HQen, HQ_2en, HQetox and HQ_2etox provided some additional insight into the speciation of the systems. ESI MS data were reported in Table 2. Solutions of the complexes at M/L molar ratios of 1:1, 1:2, and 2:1, in the pH range from 4 to 8, were analyzed.

For the systems in which L = HQen and M = Zn^{2+} or Cu^{2+}, $[MLH_{-1}]^+$ was the predominant species detected in the spectra. The $[ML_2H_{-2}] + H^+$ (with M = Zn^{2+} or Cu^{2+}) and $[ML_2H_{-2}] + K^+$ (only for Zn^{2+}) species appeared only with low intensity across all the pH values and M/L ratios explored (Figs. S27, S28).

In the Zn^{2+} or Cu^{2+} complexes of HQetox, the $[MLH_{-1}]^+$ was exclusively observed under all M/L ratios investigated (Figs. S29, S30).

For the system L = HQ_2en and M = Cu^{2+}, the spectra indicated that $[MLH_{-1}]^+$ was the most abundant species, while a bimetallic species $[M_2L_2H_{-2}] + H^+$ was present only in low intensity under all tested conditions (Fig. S31).

For the HQ_2en/Zn^{2+} system, the $[MLH_{-1}]^+$ species was more abundant at pH 5, while the dimeric species $[M_2L_2H_{-4}] + H^+$ became more prominent at neutral pH (Fig. S32). Additionally, the ESI-MS data

Table 2
ESI-MS data of the Cu^{2+} and Zn^{2+} complexes with HQen, HQetox, HQ_2en, and HQ_2etox.

Ligand (L)	Species	Formula	Calculated (*m/z*)	Experimental (*m/z*)
HQen	$[CuLH_{-1}]^+$	$[C_{12}H_{14}N_3OCu]^+$	279.1	279.3
	$[CuL_2H_{-2}] + H^+$	$[C_{24}H_{29}N_6O_2Cu]^+$	496.2	496.1
	$[ZnLH_{-1}]^+$	$[C_{12}H_{14}N_3OZn]^+$	280.1	280.4
	$[ZnL_2H_{-2}] + H^+$	$[C_{24}H_{29}N_6O_2Zn]^+$	497.2	497.4
	$[ZnL_2H_{-2}] + K^+$	$[C_{24}H_{28}N_6O_2ZnK]^+$	535.1	535.1
HQ_2en	$[CuLH_{-2}] + H^+$	$[C_{22}H_{21}N_4O_2Cu]^+$	436.2	436.3
	$[Cu_2L_2H_{-4}] + H^+$	$[C_{44}H_{41}N_8O_4Cu_2]^+$	871.2	871.4
	$[ZnLH_{-2}] + H^+$	$[C_{22}H_{21}N_4O_2Zn]^+$	437.1	437.4
	$[ZnLH_{-2}] + Na^+$	$[C_{22}H_{20}N_4O_2ZnNa]^+$	459.1	459.0
	$[Zn_2L_2H_{-4}] + H^+$	$[C_{44}H_{41}N_8O_4Zn_2]^+$	873.2	873.2
	$[ZnL_2H_{-2}] + H^+$	$[C_{44}H_{43}N_8O_4Zn]^+$	811.3	811.3
HQ_2etox	$[CuLH_{-2}] + H^+$	$[C_{26}H_{29}N_4O_4Cu]^+$	524.2	524.3
	$[CuLH_{-2}] + Na^+$	$[C_{26}H_{28}N_4O_4CuNa]^+$	546.2	546.3
	$[Cu_2L_2H_{-4}] + H^+$	$[C_{52}H_{57}N_8O_8Cu_2]^+$	1047.4	1047.1
	$[ZnLH_{-2}] + H^+$	$[C_{26}H_{29}N_4O_4Zn]^+$	525.2	525.2
	$[ZnLH_{-2}] + Na^+$	$[C_{26}H_{28}N_4O_4ZnNa]^+$	547.1	547.3
	$[ZnL_2H_{-1}]^+$	$[C_{52}H_{59}N_8O_8Zn]^+$	987.4	987.2
	$[Zn_2L_2H_{-4}] + H^+$	$[C_{52}H_{57}N_8O_8Zn_2]^+$	1049.3	1049.3
HQetox	$[CuLH_{-1}]^+$	$[C_{16}H_{22}N_3O_3Cu]^+$	367.1	367.3
	$[ZnLH_{-1}]^+$	$[C_{16}H_{22}N_3O_3Zn]^+$	368.1	368.3

revealed the formation of the ML_2 complex of Zn^{2+} at pH 5 and the Na^+ adduct of the ML complex at pH 7 (Fig. S32).

In Zn^{2+} and Cu^{2+} HQ_2etox complexes, a similar trend of the HQ_2en systems was found and the same species ML_2H_{-2} were identified at all M/L molar ratios explored. $[CuLH_{-2}] + H^+$ was the dominant species at pH 7, while $[Cu_2L_2H_{-4}] + H^+$ increases in intensity at pH 8 (Fig. S33). The Na^+ adduct of ML complex was also detected under the same pH conditions for the HQ_2etox/Cu^{2+} system (Figs. S33). The complex $[ZnLH_{-2}] + H^+$ showed higher intensity at pH 7 with its Na^+ adduct ($[ZnLH_{-2}] + Na^+$) (Fig. S34). Under neutral pH conditions, even the dimeric species $[Zn_2L_2H_{-4}] + H^+$ was also observed, whereas $[ZnL_2H_{-1}]^+$ species was only identified at low intensity at pH 8 (Fig. S34).

The main species detected by ESI-MS are consistent with those identified through spectroscopic titrations for all the ligands. ML_2 species were also detected in the ESI-MS spectra for HQ_2etox and HQ_2en. The M_2L species determined for HQ_2en and HQ_2etox by UV–vis spectroscopy was not detected in the ESI-MS spectra under the conditions explored. Due to its +2 charge, the species may be difficult to observe by ESI-MS, or a higher M/L ratio may be necessary to promote its formation. However, excess metal may cause precipitation of metal hydroxide, so we did not investigate this condition further. The species M_2L_2 for dimeric HQ derivatives was detected only at low intensity in ESI-MS spectra.

2.4. Antiproliferative activity

The antiproliferative activity of the derivatives was also tested in the presence of zinc(II) or copper(II) in A2780 and MDA-MB-231 cell lines (Table 3). The graphical representation of IC_{50} values is shown in Fig. S35. IC_{50} values higher than 30 μM were considered pharmacologically irrelevant. Data were compared to those of 8-HQ, which we previously studied in A2780 [58].

The data showed that HQ_2en was the most effective derivative (6.7 μM in A2780), similar to other 8-HQ derivatives [44].

IC_{50} values in both cell lines with HQ_2etox alone and in the presence of the metal ions were greater than 30 μM.

These results show that the HQ_2etox and HQetox derivatives were the least toxic in all the cell lines. The behavior of the new ligands studied in this work differs from that of other HQs, such as 8-HQ and CQ reported in Table 3 for comparison. For 8-HQ and CQ, IC_{50} significantly decreased in the presence of metal ions such as copper(II) [58], while for the new ligands, the complexation reduced their toxicity as reported for chelators such as TPEN [59,60].

The new ligands exhibit higher stability constants with copper and zinc than simple 8-HQ and this may induce a different toxicity mechanism. In Table S2, overall stability constants and IC_{50} values are summarized. Data suggest that stronger chelation alone cannot fully account for the observed biological activity. HQ_2en has the highest stability constants for Zn^{2+} and Cu^{2+}, and it is also the most effective inhibitor of cell proliferation. It is plausible to hypothesize that HQen and HQ_2en act predominantly as chelators rather than ionophores. The chelation of essential metal ions can disrupt intracellular metal homeostasis, leading to toxic effects on cells. However, this effect was reduced upon the addition of copper(II) and zinc(II). This diminished efficacy may also be attributed to the formation of stable metal–ligand complexes, which lower the availability of the free ligand and limit its interaction with cellular targets.

In the case of HQ_2etox and HQetox, which form also very stable Zn^{2+} and Cu^{2+} complexes (Table 1), the linker may confer polarity to the ligands, reducing their cellular uptake. The antiproliferative activity becames pharmacologically irrelevant in the presence of copper or zinc ions ($IC_{50} > 30$ μM).

2.5. Antimicrobial activity

The antimicrobial activity of the compounds was evaluated using the broth microdilution method. MIC values are summarized in Table 4 and the corresponding graphical representation is reported in Fig. S36.

The aim of the co-treatment experiment was to evaluate the potential modulatory effect of Cu^{2+} or Zn^{2+} ions on the antimicrobial efficacy of HQen, HQ_2en, HQetox and HQ_2etox against four bacterial strains. HQ_2etox was excluded from the MIC table due to its substantially lower antibacterial activity compared to other compounds.

Under standard conditions, HQ_2en was the most effective compound, exhibiting a MIC of 16 μg/mL against all tested strains, comparable to the activity of 8-HQ [23]. HQen showed moderate antimicrobial activity, with MIC values of 256 μg/mL for *S. aureus* and *E. coli*, and 512 μg/mL for *P. aeruginosa* and *E. faecalis*. Finally, HQetox showed MIC values of 256 μg/mL for all tested strains, except for *P. aeruginosa*, which showed a MIC of 512 μg/mL. These findings indicated that HQ_2en possessed broad-spectrum antibacterial activity with low MIC values, whereas HQen and HQetox were significantly less potent under the same conditions.

In the co-treatment experiments with copper(II) and zinc(II), several notable patterns emerged. A general trend of reduced antibacterial efficacy was observed for all compounds, evidenced by increased MIC values. This behavior differs from that reported for 8-HQ, which increases its antibacterial activity in the presence of Cu^{2+} [52].

In *S. aureus*, co-treatment with HQ_2en with Cu^{2+} and Zn^{2+} yielded MICs of 64 μg/mL and > 64 μg/mL, respectively, indicating diminished activity compared to HQ_2en alone. HQen, in combination with copper or zinc, displayed even higher MIC values of 1024 μg/mL for both metals, indicating a strong antagonistic effect. Similarly, HQetox also showed no improvement when combined with metals.

In *E. coli*, HQ_2en MICs increased to >64 μg/mL with both metal ions, further supporting the trend of reduced antimicrobial activity. Co-treatment of HQen with copper or zinc resulted in MICs of 2048 μg/mL and MBCs >2048 μg/mL, respectively, while HQetox displayed MICs of 512 μg/mL and MBCs >512 μg/mL under both conditions, indicating no improvement over single-agent treatment.

The pattern was similar for *P. aeruginosa:* MICs raised to >64 μg/mL

Table 3
IC_{50} values (μM) of HQ_2en, HQen, HQ_2etox and HQetox alone and in the presence of Cu^{2+} (20 μM) or Zn^{2+} (50 μM).

Compound	Cell line					
	A2780			MDA-MB-231		
	L	+ Cu^{2+}	+ Zn^{2+}	L	+ Cu^{2+}	+ Zn^{2+}
HQ_2en	6.7 ± 0.9	24.1 ± 4.1	24.2 ± 1.7	19.4 ± 5.9	>30	>30
HQen	24.0 ± 3.2	30.1 ± 2.6[a]	>30	26.5 ± 5.5	>30	>30
HQ_2etox	>30	>30	>30	>30	>30	>30
HQetox	>30	>30	>30	>30	>30	>30
8-HQ [58]	2.17	0.33	ND			
CQ [58]	55.31	5.98	ND			

[a] $p < 0.01$, as compared to the treatment with HQen alone.

Table 4
MIC (μg/mL) and MBC (μg/mL, in brackets) of HQ_2en, HQen and HQetox alone and in the presence of Cu^{2+} or Zn^{2+} (100 μM) against reference bacterial strains.

	HQ_2en			HQen			HQetox		
	L	+ *Cu* (MBC)	+ *Zn* (MBC)	L	+ *Cu* (MBC)	+ *Zn* (MBC)	L	+ *Cu* (MBC)	+ *Zn* (MBC)
S. aureus	16	64 (>64)	>64 (>64)	256	1024 (>1024)	1024 (2048)	256	>512	512 (512)
E. coli	16	>64 (>64)	>64 (>64)	512	2048 (>2048)	2048 (>2048)	256	512 (>512)	512 (>512)
P. aeruginosa	16	>64 (>64)	>64 (>64)	512	2048 (>2048)	2048 (2048)	512	512 (512)	512 (512)
E. faecalis	16	4 (>512)	>64 (>512)	256	128 (>512)	>2048 (>2048)	256	512 (>512)	>512 (>512)

for HQ_2en, 2048 μg/mL for HQen and 512 μg/mL for HQetox. Moreover, the MBCs for all compounds in combination with either metal increased, with HQ_2en exceeding 64 μg/mL, HQen reaching 2048 μg/mL for zinc co-treatment and over 2048 μg/mL for copper co-treatment, and HQetox showed MBCs of 512 μg/mL in both metal conditions.

The most intriguing results were obtained with *E. faecalis*, particularly when HQ_2en was combined with copper. While the MIC was 4 μg/mL, the MBC rose to over 512 μg/mL. The same pattern was observed for HQen, where the MIC value decreased to 128 μg/mL, but the MBC value increased to over 512 μg/mL, suggesting a potential bacteriostatic effect of the copper complex, specifically against this bacterium.

Conversely, HQetox demonstrated the same pattern observed with other strains, where the addition of metals resulted in MIC values of 512 μg/mL and MBC values exceeding 512 μg/mL for both metals (Table 4).

The data suggest that the antimicrobial activity of HQ_2en was generally diminished in the presence of the metal ions. The behavior of HQ_2en in bacteria is similar to that found in cancer cells. HQ_2en is the most effective ligand and it showed the highest toxicity for cancer cells and bacteria (Table S2).

HQen and HQEtox, already less effective as stand-alone agents, showed consistently diminished antimicrobial properties in the presence of copper(II) or zinc(II). The only notable exception was *E. faecalis* treated with copper, which showed a decrease in the MIC value of HQ_2en and HQen. This behavior suggests that metal ion chelation may act as a mechanism of toxicity of the ligands in the bacterial strains investigated.

These findings highlighted the potential antibacterial properties of HQ_2en, which showed broad-spectrum and low MIC values across all tested strains.

3. Experimental

3.1. Materials and methods

Commercially available reagents were used directly unless otherwise noted. 8-Hydroxyquinoline-2-carboxaldehyde (HQCA) was purchased from Sigma-Aldrich; Boc-ethylenediamine (Boc-en), ethylenediamine (en), and 1,2-Bis(2-aminoethoxy)ethane (etox) were obtained from TCI (Tokyo Chemical Industry Co., Ltd).

Thin-layer chromatography (TLC) was performed on silica gel plates (Merck 60-F254).

The purity of the ligands (> 95 %) was verified with HPLC (column reversed-phase C18, eluent $H_2O \rightarrow CH_3CN$).

All ligand stock solutions were prepared by dissolving properly weighed amounts in a 25–90 % *v*/v MeOH/H_2O mixed solvent. Solutions for spectrophotometric titrations were prepared by diluting the stock into a 10 mM aqueous solution of 3-N-morpholinopropanesulfonic acid (MOPS, pH 7.4), ensuring that the final methanol concentration was always below 3 %. Copper and zinc stock solutions were prepared by solubilizing $Cu(ClO_4)_2$ or $Zn(ClO_4)_2$ in water and titrating the resulting solutions with standardized EDTA.

3.2. NMR spectroscopy

NMR spectra were recorded on a Bruker Avance™ 400 spectrometer at 25 °C. Chemical shift values were referenced to the solvent signal or TMS. 8-HQ atoms were numbered according to standard IUPAC nomenclature [61].

3.3. Mass spectrometry

ESI-MS measurements were performed using a linear ion trap electrospray mass spectrometer (LTQ, Thermo Finnigan, Milan, Italy). The samples were introduced by direct infusion at a flow rate of 5 μL/min into the electrospray ion source (ESI). After appropriate tuning processes to optimize the signal-to-noise ratio, mass spectra were acquired in positive ion mode using a spray voltage of 5 kV and introduced into the mass spectrometer through a heated ion transfer tube (275 °C). The sheath gas flow rate and the auxiliary gas flow rate were set to 10.0 and 3.0 (arbitrary units), respectively. Mass spectrometer calibration was performed using the Pierce® LTQ Velos ESI Positive Ion calibration mixture (Thermo Fisher Scientific). MS data acquisition was performed using Xcalibur software v.2.2.0.48 (Thermo Fisher Scientific).

Sample solutions of metal complexes were diluted in water and/or methanol for LC/MS analysis (OPTIMA® LC/MS grade, Fisher Scientific, Milan, Italy) with 0.1 % formic acid, and the pH was adjusted with NaOH. Copper(II) and zinc(II) complexes for ESI-MS studies were prepared by adding a solution of copper(II) or zinc(II) to water/methanol solutions of the ligands. Solutions of the complexes at 1:1, 1:2, and 2:1 M/L molar ratios, in the pH range from 4 to 8, were analyzed.

ESI-HRMS measurements were performed using an Orbitrap Fusion Tribrid (Q-OT-qIT) mass spectrometer (ThermoFisher Scientific, Bremen, Germany). The samples were introduced by direct infusion at a flow rate of 3 μL/min into the ESI ion source (Thermo Scientific). After optimizing the signal-to-noise ratio through appropriate tuning processes, mass spectra were acquired in positive ion mode under the following conditions: spray voltage, 3.8 kV; capillary temperature, 275 °C; sheath gas and auxiliary gas, 6.0 and 2.0 (arbitrary units), respectively. Mass spectrometer calibration was carried out using the PierceTM FlexMixTM Calibration Solution (Thermo Fisher Scientific, A39239).

MS data acquisition was performed using the Xcalibur v. 4.6.67.17 software (Thermo Fisher Scientific). Simulated isotope distributions were made using the Molecular Mass Calculator (MS Tools-EPFL, https://ms.epfl.ch/applications/theoretical-calculations/).

3.4. UV–Vis spectroscopy and spectroscopic titrations

UV–Vis spectra were recorded with a Cary 3500 UV-Vis spectrophotometer equipped with a Peltier temperature control module. The metal complexes were prepared by mixing a metal ion solution with the ligand in a 1:1 M/L molar ratio.

UV–Vis competition titrations were performed at 25 °C in a buffered aqueous medium (pH 7.4, 10 mM MOPS) using an Agilent 8453 diode-array spectrophotometer. In the case of HQen, HQetox and HQ_2etox, increasing amounts of a standardized EDTA solution ($3.8–8.5 \times 10^{-4}$ M) were added with a precision burette into the cell containing 2 mL of either a M/L 1:1 (L = HQen or HQetox; $C_L = 4.9–6.0 \times 10^{-5}$ M) or a M/L 2:1 (L = HQ_2etox, $C_L = 2.0–3.0 \times 10^{-5}$ M) complex solution. For HQ_2en, increasing amounts of a M^{2+}-EDTA 1:1 complex solution ($C_{EDTA} = 3.0 \times 10^{-4}$ –1.0×10^{-3} M) were added into the cell containing 2 mL of a $1.8–3.0 \times 10^{-5}$ M ligand solution. Various titrant/titrate ratios were

explored to optimize the formation of each complex species during the titration. 60–70 spectra were recorded for each titration, and at least three independent runs were collected for each system. Spectra were analyzed with Hyperquad, which allows for a multi-wavelength and multi-titration treatment of the data [62]. The conditional stability constant for the M^{2+}-EDTA complexes (log $K_{Cu\text{-}EDTA}$ = 15.9; log $K_{Zn\text{-}EDTA}$ = 13.63) at pH 7.4 was calculated from the literature values [26] and included in the model as a fixed/known parameter.

3.5. Synthesis of 2-(((2-aminoethyl)amino)methyl)quinolin-8-ol (HQen)

HQCA (0.05 g, 0.289 mmol), Boc-en (46 μL, 0.289 mmol) and CH_3ONa (0.03 g, 0.578 mmol) were dissolved in 3 mL of methanol at 25 °C, under stirring.

After 1 h, $NaBH_4$ (0.055 g, 1.44 mmol) was added to the solution and the mixture was refluxed. After 5 h, the crude product was isolated and treated with trifluoroacetic acid overnight to remove the Boc protecting group. The final product was isolated by reversed-phase flash chromatography (eluent H_2O/CH_3CN, linear gradient 0–80 % CH_3CN). The product was eluted at 30 % CH_3CN.

TLC: R_f = 0.24, PrOH/AcOEt/H_2O/NH_3 4:3:1:2. Yield: 60 %.

ESI-HRMS *m/z* [Found (Theoretical)] = 218.1265 (218.1293) $(L + H)^+$; 240.1089 (240.1113) $(L + Na)^+$.

^{1}H NMR (400 MHz, D_2O, pD = 5.0 DCl): δ 8.40 (d, *J* = 8.6 Hz; 1H, H-4), 7.53 (d, *J* = 8.6 Hz; 1H, H-3), 7.51 (d, *J* = 5.7 Hz; 1H, H-7), 7.51 (d, *J* = 3.2 Hz; 1H, H-5), 7.24 (dd, J_1 = 5.7 Hz, J_2 = 3.2 Hz; 1H, H-6), 4.69 (s, 2H, CH_2), 3.60 (t, *J* = 6.8 Hz; 2H, CH_2NH), 3.48 (t, *J* = 6.8 Hz; 2H, CH_2NH_2).

^{13}C NMR (100 MHz, D_2O, pD = 5.0 DCl): δ 150.79 (C-8), 149.46 (C-2), 139.29 (C-10), 136.63 (C-4), 128.78 (C-9), 128.48 (C-3), 120.42 (C-6), 119.48 (C-5), 112.88 (C-7), 50.97 (CH_2 py), 44.40 (CH_2NH), 35.72 (CH_2NH_2).

3.6. Synthesis of 2,2′-((ethane-1,2-diylbis(azanediyl))bis(methylene))bis(quinolin-8-ol) (HQ_2en)

HQCA (0.05 g, 0.289 mmol), en (10 μL, 0.145 mmol) and CH_3ONa (0.03 g, 0.578 mmol) were dissolved in 3 mL of methanol at 25 °C under stirring. After 5 h, $NaBH_4$ (0.055 g, 1.44 mmol) was added, and the reaction was stirred for an additional 12 h. The reaction produced a yellow precipitate, which was separated from the solution by filtration. The product was isolated by reversed-phase flash chromatography (eluent H_2O/CH_3OH, linear gradient 0–100 % CH_3CN).

TLC: R_f = 0.68, PrOH/AcOEt/H_2O/NH_3 2:2:3:3. Yield: 70 %.

ESI-HRMS *m/z* [Found (Theoretical)] = 375.1784 (375.1821) $(L + H)^+$; 397.1598 (397.1640) $(L + Na)^+$.

^{1}H NMR (400 MHz, CD_3OD): d 8.16 (d, *J* = 8.5 Hz; 2H, H-4), 7.58 (d, *J* = 8.5 Hz 2H, H-6), 7.36 (d, J = 8.5 Hz, 2H, H-3), 7.27 (d, *J* = 8.5 Hz; 2H, H-5), 7.04 (dd, J_1 = 8.5 Hz, J_2 = 1.2 Hz; 2H, H-7), 4.07 (s, 4H, CH_2 py), 2.92 (s; 4H, CH_2 en).

^{13}C NMR (100 MHz, CD_3OD): δ 148.7 (C-2), 145.7 (C-8), 136.01 (C-10), 135.59 (C-4), 126.64 (C-6), 117.21 (C-7 and C-3), 110.37 (C-5), 58.02 (CH_2NH), 45.98 (CH_2NH).

3.7. Synthesis of 2,2′-(5,8-dioxa-2,11-diazadodecane-1,12-diyl)bis(quinolin-8-ol) (HQ_2etox)

HQCA (0.05 g, 0.289 mmol), etox (21 μL, 0.145 mmol) and CH_3ONa (0.03 g, 0.578 mmol) were dissolved in 2 mL of ethanol under stirring at 25 °C. After 5 h, $NaBH_4$ (0.055 g, 1.44 mmol) was added and the reaction mixture was stirred for 12 h. The product was isolated by reversed-phase C18 flash chromatography eluted with H_2O/CH_3CN (linear gradient 0–100 % CH_3CN). The product was eluted at 100 % CH_3CN.

TLC: R_f = 0.58, PrOH/AcOEt/H_2O/NH_3 2:2:3:1. Yield: 30 %.

ESI-HRMS *m/z* [Found (Theoretical)] = 463.2303 (463.2345) $(L + H)^+$; 485.2123 (485.2165) $(L + Na)^+$.

^{1}H NMR (400 MHz, CD_3OD): δ 8.00 (d, *J* = 8.6 Hz, 2H, H-4), 7.33 (d, *J* = 8.2. Hz, 2H, H-6), 7.23 (m, 4H, H-3 and H-7), 7.03 (d, *J* = 8.6 Hz, H-5), 4.02 (s, 4H, CH_2 py), 3.49 (m, 8H, CH_2O), 2.87 (t, *J* = 4.7 Hz; 4H, CH_2NH).

^{13}C NMR (100 MHz, CD_3OD): δ 156.42 (C-2), 152.63 (C-8), 139.29 (C-10), 136.12 (C-4), 127.67 (C-9), 126.59 (C-6), 120.51 (C-3 or C-7), 117.21 (C-7 or C-3), 110.53 (C-5), 69.87 (CH_2O), 69.49 (CH_2O), 53.24 (CH_2NH), 47.87 (CH_2NH).

3.8. Synthesis of 2-(((2-(2-(2-aminoethoxy)ethoxy)ethyl)amino)methyl)quinolin-8-ol (HQetox)

The product was synthesized as reported for HQ_2etox using a different molar ratio: HQCA (0.05 g, 0.289 mmol), etox (85 μL, 0.577 mmol) and CH_3ONa (0.03 g, 0.578 mmol). After 5 h, $NaBH_4$ (0.055 g, 1.44 mmol) was added and the reaction mixture was stirred for 12 h. The derivative was isolated by reversed-phase C18 flash chromatography using a linear gradient of H2O/CH3CN (0–100 % CH_3CN). The product was collected at 80 % CH_3CN.

TLC: R_f = 0.54, PrOH/AcOEt/H_2O/NH_3 4:3:2:1. Yield: 40 %.

ESI-HRMS *m/z* [Found (Theoretical)] = 306.2000 (306.1818) $(L + H)^+$; 328.1819 (328.1637) $(L + Na)^+$.

^{1}H NMR (400 MHz, CD_3OD): δ 8.17 (d; *J* = 8.5 Hz; 1H, H-4), 7.42 (d; *J* = 8.5 Hz; 1H, H-3), 7.39 (t; J_1 = 8.5 Hz; 1H, H-6), 7.31 (dd; J_1 = 8.5 Hz, J_2 = 1.3 Hz; 1H, H-5), 7.08 (dd; J_1 = 8.5 Hz, J_2 = 1.3 Hz; 1H, H-7), 4.10 (s, 2H, CH_2 py), 3.68 (t, *J* = 5.3 Hz; 2H, CH_2O), 3.65 (m, 4H, CH_2O), 3.55 (t, *J* = 5.3 Hz; 2H, CH_2O), 2.89 (t, *J* = 5.3 Hz; 2H, CH_2NH), 2.81 (t, *J* = 5.3 Hz; 2H, CH_2NH2).

^{13}C NMR (100 MHz, CD_3OD): δ 158.19 (C-8), 154.65 (C-2), 139.45 (a), 137.82 (C-4), 129.42 (b), 128.31 (C-3), 122.08 (C-6), 118.57 (C-5), 112.22 (C-7), 72.58 (CH_2 py), 71.31 (CH_2O), 71.24 (CH_2O), 71.07 (CH_2O), 55.15 (CH_2O), 49.52 (CH_2NH), 41.78 (CH_2NH_2).

3.8.1. Antiproliferative activity assay

Human tumor cell lines A2780 (ovary, adenocarcinoma) and MDA-MB-231 (breast, carcinoma) were plated into flat-bottomed 96-well microtiter plates at the appropriate numbers in 180 μL per well of complete media (RPMI 1640 for A2780, DMEM for MDA-MB-231), added with 10 % fetal bovine serum (FBS) and 1 % penicillin-streptomycin (all media and additives were obtained from EuroClone spa, Pero, MI, Italy) and 20 μM Cu^{2+} or 50 μM Zn^{2+} when required. Plates were then centrifuged and after 6–7 h, 20 μL of the appropriate solvent (FBS plus DMSO at different concentrations depending on the specific solubility) containing five 1:4 concentrations of the compounds starting from 50 μM were administered to cells. HQ derivatives alone and in the presence of Cu^{2+} and Zn^{2+} were studied. After 3 days of treatment (performed in duplicate) the cells, resuspended in 200 μl of medium per well, were supplemented with 50 μL of MTT solution (3-(4,5-dimethylthiazol-2-yl)-2,5-diphenyltetrazolium bromide; 2 mg/mL in PBS; Sigma, St. Louis, MO, USA). The plates were then still incubated for an additional 4 h at 37 °C. Following incubation, the cells were centrifuged at 275 ×*g* for 2 min. The supernatant was then carefully aspirated, and 100 μL of pure DMSO was added to each well. Formazan crystals were fully solubilized by gentle shaking after a 30-min incubation at room temperature. The concentrations inhibiting 50 % cell growth (IC_{50}) were calculated based on the analysis of the concentration-response curves. Each experiment was repeated 4–6 times.

3.8.2. Antibacterial activity assay

The antimicrobial activity of the compounds was tested against four bacterial strains: *Staphylococcus aureus* ATCC 25213, *Pseudomonas aeruginosa* ATCC 27853, *Enterococcus faecalis* ATCC 29212, and *Escherichia coli* ATCC 25922.

The minimum inhibitory concentration (MIC) for each compound was determined using the broth microdilution method. The MIC was

defined as the lowest concentration at which no visible bacterial growth was observed. To evaluate bactericidal activity, the minimum bactericidal concentration (MBC) was also determined. For samples showing complete inhibition of growth, aliquots from wells without visible turbidity were subcultured onto agar plates and incubated for 24 h. The MBC was defined as the lowest concentration at which no colony growth was detected. Bacterial strains were cultured overnight on Mueller-Hinton (MH) agar plates at 37 °C under aerobic conditions. From these cultures, a 0.5 McFarland standard suspension was prepared for each strain and further diluted to achieve a final inoculum of approximately 1.0×10^6 CFU/mL. In parallel, stock solutions of the compounds were prepared by dissolving them in MH broth and serial dilutions were made to obtain final concentrations ranging from 512 to 16 μg/mL.

Subsequently, an aliquot of the bacterial suspension was added to each well of the microdilution plate, yielding a final bacterial concentration of 1.0×10^5 CFU/mL. Wells containing only the bacterial inoculum served as positive controls, while wells containing only MH broth served as negative controls. A second set of experiments was conducted to assess the effect of metal co-treatment on the antibacterial activity of the same compounds. In these experiments, 100 μM Cu^{2+} or Zn^{2+} solutions were added to each well along with the compound of interest. Each experimental condition was tested in quadruplicate to ensure reproducibility. The plates were incubated at 37 °C for 24 h.

4. Conclusions

New hydroxyquinolines were synthesized, characterized and evaluated for their metal complex stability and biological activity.

The dimeric derivatives, with the hydroxyquinoline units linked by the diaminoethane chain, formed highly stable complexes with copper (II) ($\log\beta_{CuL} = 19.2$) and zinc(II) ($\log\beta$ ZnL = 15.17), and can also form bimetallic species with two hydroxyquinoline coordination sites that are almost independent and exhibit comparable stability constants ($\log\beta_{Cu2L} = 33.3$, $\log\beta_{Zn2L} = 29.88$) at physiological pH. A similar behavior was observed for the diaminodioxaoctane chain. Notably, the functionalization of the 8-hydroxyquinoline ring can efficiently modulate the toxicity of the derivatives. This is particularly relevant given the longstanding interest in hydroxyquinoline-based ligands for their metal-chelating capacity and biological versatility. Remarkably, the ethylenediamine 8-hydroxyquinoline dimeric derivative forms the most stable complexes and exhibits the highest cytotoxicity. It exhibited micromolar antiproliferative activity in cancer cells (IC_{50} 6.7 μM in A2780 and 19.4 μM in MDA-MB-231) and good antibacterial activity (MIC 16 μg/mL in *S. aureus*, *E. coli*, *P. aeruginosa* and *E. faecalis*), consistent with the performance of 8-hydroxyquinoline. These biological activities were reduced in the presence of copper(II) or zinc(II), unlike simple 8-hydroxyquinoline. This behavior suggests that HQen and HQ_2en can act predominantly as chelators rather than ionophores. The chelation of essential metal ions may disrupt intracellular metal homeostasis, thereby leading to toxicity.

Interestingly, the dimer and monomer with the diaminodioxaoctane chain showed the lowest antiproliferative activity ($IC_{50} > 30$ μM and MIC >2048 μg/mL).

The low toxicity of the two ligands for cancer cells and bacterial strains, also in the presence of metal ions, together with their ability to coordinate with high stability constants biologically relevant metal ions such as Cu^{2+} and Zn^{2+}, makes the new ligands ideal for studying metal-dependent cellular processes, metal-based therapeutic strategies and other applications, such as chelation therapy.

This finding highlights that ligand design critically influences metal complexation, demonstrating how new chelating agents can modulate metal bioavailability. Such control has broad implications in medicinal inorganic chemistry for developing metal-based drugs that either deprive cells of essential metals (as in antimicrobial or anticancer strategies) or fine-tune metal homeostasis for therapeutic benefit (neuroprotection, treatment of metal overload).

CRediT authorship contribution statement

Roberta Panebianco: Writing – review & editing, Writing – original draft, Methodology, Investigation, Formal analysis, Data curation. **Giuseppina D.G. Santonoceta:** Writing – original draft, Methodology, Investigation, Formal analysis, Data curation. **Roberta Borrelli:** Methodology, Investigation, Data curation. **Maria G.G. Pittalà:** Writing – original draft, Methodology, Investigation, Data curation. **Rosaria Saletti:** Writing – original draft, Methodology, Investigation, Data curation. **Carmelo Sgarlata:** Writing – review & editing, Writing – original draft, Validation, Methodology, Investigation, Formal analysis. **Maurizio Viale:** Writing – review & editing, Writing – original draft, Methodology, Investigation, Formal analysis, Data curation. **Salvatore Furnari:** Writing – original draft, Methodology, Investigation, Data curation. **Virginia Fuochi:** Writing – original draft, Methodology, Investigation, Data curation. **Pio M. Furneri:** Writing – original draft, Methodology, Investigation, Data curation. **Tommaso Mecca:** Writing – original draft, Methodology, Investigation. **Graziella Vecchio:** Writing – review & editing, Writing – original draft, Supervision, Project administration, Investigation, Funding acquisition.

Declaration of competing interest

There are no conflicts to declare.

Acknowledgements

We thank the Italian Ministry of Health (Ricerca Corrente 2024, recipient Maurizio Viale), EU funding within the NextGeneration EU-MUR PNRR Extended Partnership initiative on Emerging Infectious Diseases (Project no. PE00000007, INF-ACT), PRIN (Project no. 2022JXSA9C, SPlat-G) and University of Catania (Pia.ce.ri. 2024-26 – "Interactive" project) for financial support. We also acknowledge the Bio-Nanotech Research and Innovation Tower (BRIT) for providing access to the Orbitrap Fusion mass spectrometer.

Appendix A. Supplementary data

Supplementary data to this article can be found online at https://doi.org/10.1016/j.jinorgbio.2025.113138.

Data availability

The data supporting this article have been included as part of the Supplementary Information.

References

[1] Metal Chelation in Medicine, The Royal Society of Chemistry, 2016.
[2] K. Bajbouj, J. Shafarin, M. Hamad, Technol. Cancer Res. Treat. 17 (2018), 1533033818764470.
[3] M. Balali-Mood, N. Eizadi-Mood, H. Hassanian-Moghaddam, L. Etemad, M. Moshiri, M. Vahabzadeh, M. Sadeghi, Heliyon 11 (2025) e42696.
[4] M.T. Ma, P.J. Blower. Metal Chelation in Medicine, The Royal Society of Chemistry, 2016, pp. 260–312. https://doi.org/10.1039/9781782623892-00260.
[5] Z. Salimi, M. Afsharinasab, M. Rostami, Y. Eshaghi Milasi, S.F. Mousavi Ezmareh, F. Sakhaei, M. Mohammad-Sadeghipour, S.M. Rasooli Manesh, Z. Asemi, Ann. Med. Surg. 86 (2024) 2759.
[6] Y. Liu, M. Nafees, M. Hanif, ChemBioChem 26 (2025) e202500026.
[7] R. Singh, A. Panghal, K. Jadhav, A. Thakur, R.K. Verma, C. Singh, M. Goyal, J. Kumar, A.G. Namdeo, Mol. Neurobiol. 61 (2024) 10916–10940.
[8] Z. Jiang, Q. You, X. Zhang, Eur. J. Med. Chem. 165 (2019) 172–197.
[9] A. El Ayadi, J.R. Salsbury, P. Enkhbaatar, D.N. Herndon, N.H. Ansari, Redox Biol. 45 (2021) 102034.
[10] M.M. Leitão, A.S.C. Gonçalves, J. Moreira, C. Fernandes, F. Borges, M. Simões, A. Borges, Eur. J. Med. Chem. 283 (2025) 117163.
[11] L. Principe, G. Vecchio, G. Sheehan, K. Kavanagh, G. Morroni, V. Viaggi, A. di Masi, D.R. Giacobbe, F. Luzzaro, R. Luzzati, S. Di Bella, Microb. Drug Resist. Larchmt. N 26 (2020) 1133–1143.
[12] G. Dhanda, Y. Acharya, J. Haldar, ACS Omega 8 (2023) 10757–10783.

[13] J. Benadiba, C. Rosilio, M. Nebout, V. Heimeroth, Z. Neffati, A. Popa, D. Mary, E. Griessinger, V. Imbert, N. Sirvent, J.-F. Peyron, Leuk. Lymphoma 58 (2017) 1433–1445.
[14] C.E. Housecroft, E.C. Constable, Chem. Commun. 56 (2020) 10786–10794.
[15] H.-Y. Yin, J. Tang, J.-L. Zhang, Eur. J. Inorg. Chem. 2017 (2017) 5085–5093.
[16] E.S. Al-Farraj, S.K. Alharbi, M. Feizi-Dehnayebi, B.H. Asghar, N. Alahmadi, T.N. A. Eskander, M.A. Alghamdi, A.M. Abu-Dief, Appl. Organomet. Chem. 39 (2025) e70273.
[17] R. Gupta, V. Luxami, K. Paul, Bioorg. Chem. 108 (2021) 104633.
[18] L. Côrte-Real, V. Pósa, M. Martins, R. Colucas, N.V. May, X. Fontrodona, I. Romero, F. Mendes, C. Pinto Reis, M.M. Gaspar, J.C. Pessoa, É.A. Enyedy, I. Correia, Inorg. Chem. 62 (2023) 11466–11486.
[19] C. Bissani Gasparin, D.A. Pilger, ChemistrySelect 8 (2023) e202204219.
[20] L. Li, H. Wu, J. Wang, Z. Ji, T. Fang, H. Lu, L. Yan, F. Shen, D. Zhang, Y. Jiang, T. Ni, J. Med. Chem. 66 (2023) 16364–16376.
[21] A. Bhagwat, A. Butts, E. Greve, Y. Cheung, E. Melief, J. Gomez, D.T. Hung, T. Parish, ACS Infect. Dis. 10 (2024) 3692–3698.
[22] X. Zhou, J. Inorg. Biochem. 238 (2023) 112051.
[23] R. Cherdtrakulkiat, S. Boonpangrak, N. Sinthupoom, S. Prachayasittikul, S. Ruchirawat, V. Prachayasittikul, Biochem. Biophys. Rep. 6 (2016) 135–141.
[24] R.D. Gupta, G.S. Manku, A.N. Bhat, B.D. Jain, Z. Für Anorg. Allg. Chem. 379 (1971) 312–319.
[25] J. Stary, Critical Evaluation of Equilibrium Constants Involving 8-Hydroxyquinoline and its Metal Chelates, Pergamon Press, 2013.
[26] R.M. Smith, A.E. Martell, Critical Stability Constants, Springer, US, 1989.
[27] L. Cahoon, Nat. Med. 15 (2009) 356–359.
[28] T. Tsubaki, Y. Honma, M. Hoshi, Lancet 297 (1971) 696–697.
[29] H. Schaumburg, S. Herskovitz, Neurology 71 (2008) 622–623.
[30] K.J. Barnham, A.I. Bush, Chem. Soc. Rev. 43 (2014) 6727–6749.
[31] B. Chen, J. Liu, J. Inorg. Biochem. 257 (2024) 112578.
[32] Q.-P. Qin, Z.-F. Wang, M.-X. Tan, X.-L. Huang, H.-H. Zou, B.-Q. Zou, B.-B. Shi, S.-H. Zhang, Metallomics 11 (2019) 1005–1015.
[33] Q.-M. Li, X.-Q. Huang, Q. Su, J.-M. Zhang, L.-Q. Qin, M.-X. Tan, Q.-P. Qin, Polyhedron 279 (2025) 117619.
[34] V.V. Gaensicke, S. Bachmann, L. Craciunescu, A.W. Prentice, M.J. Paterson, D. Iuga, P.J. Sadler, R.C. Marchi, Dalton Trans. 54 (2025) 5446–5457.
[35] V.F.S. Pape, N.V. May, G.T. Gál, I. Szatmári, F. Szeri, F. Fülöp, G. Szakács, É. A. Enyedy, Dalton Trans. 47 (2018) 17032–17045.
[36] V.F.S. Pape, R. Palkó, S. Tóth, M.J. Szabó, J. Sessler, G. Dormán, É.A. Enyedy, T. Soós, I. Szatmári, G. Szakács, J. Med. Chem. 65 (2022) 7729–7745.
[37] W.-Q. Ding, B. Liu, J.L. Vaught, H. Yamauchi, S.E. Lind, Cancer Res. 65 (2005) 3389–3395.
[38] P. Chen, Y. Wang, H. Tang, C. Zhou, Z. Liu, S. Gao, T. Wang, Y. Xu, S.-L. Ji, J. Pharm. Anal. 15 (2025) 101069.
[39] V.F.S. Pape, N.V. May, G.T. Gál, I. Szatmári, F. Szeri, F. Fülöp, G. Szakács, É. A. Enyedy, Dalton Trans. 47 (2018) 17032–17045.
[40] A. Ali, S. Banerjee, S. Kamaal, M. Usman, N. Das, M. Afzal, A. Alarifi, N. Sepay, P. Roy, M. Ahmad, RSC Adv. 11 (2021) 14362–14373.
[41] K.L. Summers, N.V. Dolgova, K.B. Gagnon, G.J. Sopasis, A.K. James, B. Lai, N. J. Sylvain, H.H. Harris, H.K. Nichol, G.N. George, I.J. Pickering, Metallomics 12 (2020) 1979–1994.
[42] V.F.S. Pape, R. Palkó, S. Tóth, M.J. Szabó, J. Sessler, G. Dormán, É.A. Enyedy, T. Soós, I. Szatmári, G. Szakács, J. Med. Chem. 65 (2022) 7729–7745.
[43] C. Deraeve, M. Pitié, H. Mazarguil, B. Meunier, New J. Chem. 31 (2007) 193–195.
[44] C. Deraeve, C. Boldron, A. Maraval, H. Mazarguil, H. Gornitzka, L. Vendier, M. Pitié, B. Meunier, Chem. Eur. J. 14 (2008) 682–696.
[45] V. Oliveri, G. Vecchio, Eur. J. Inorg. Chem. 2021 (2021) 1993–1999.
[46] V. Oliveri, C. Sgarlata, G. Vecchio, Chem. Asian J. 11 (2016) 2436–2442.
[47] A. Barilli, C. Atzeri, I. Bassanetti, F. Ingoglia, V. Dall'Asta, O. Bussolati, M. Maffini, C. Mucchino, L. Marchiò, Mol. Pharm. 11 (2014) 1151–1163.
[48] S.L. Srivastava, M. Prasad, Rohitashava, Spectrochim. Acta Part Mol. Spectrosc. 40 (1984) 681–685.
[49] C.-Q. Xiao, Q. Huang, Y. Zhang, H.-Q. Zhang, L. Lai, Thermochim. Acta 691 (2020) 178721.
[50] C. Sgarlata, G. Arena, R.P. Bonomo, A. Giuffrida, G. Tabbì, J. Inorg. Biochem. 180 (2018) 89–100.
[51] X. Liang, Y. Ding, L. Luo, W. Hu, F. Li, Y. Song, K. Kang, J. Mater. Sci. 60 (2025) 690–705.
[52] A. Cipurković, E. Horozić, A. Marić, L. Mekić, H. Junuzović, Open J. Appl. Sci. 11 (2021) 1–10.
[53] V.B. Kenche, I. Zawisza, C.L. Masters, W. Bal, K.J. Barnham, S.C. Drew, Inorg. Chem. 52 (2013) 4303–4318.
[54] G.H. Nancollas, M.B. Tomson, Pure Appl. Chem. 54 (1982) 2675–2692.
[55] James. Fresco, Henry. Freiser, Anal. Chem. 36 (1964) 372–375.
[56] R.L. Stevenson, Henry. Freiser, Anal. Chem. 39 (1967) 1354–1358.
[57] W. Zhang, D. Huang, M. Huang, J. Huang, D. Wang, X. Liu, M. Nguyen, L. Vendier, S. Mazères, A. Robert, Y. Liu, B. Meunier, ChemMedChem 13 (2018) 684–704.
[58] V. Oliveri, M. Viale, C. Aiello, G. Vecchio, J. Inorg. Biochem. 142 (2015) 101–108.
[59] S. Schaefer-Ramadan, M. Barlog, J. Roach, M. Al-Hashimi, H.S. Bazzi, K. Machaca, Bioorg. Chem. 87 (2019) 366–372.
[60] M. Mendivil-Perez, C. Velez-Pardo, L.M. Quiroz-Duque, A. Restrepo-Rincon, N. A. Valencia-Zuluaga, M. Jimenez-Del-Rio, BioMetals 35 (2022) 741–758.
[61] J. Kidrič, D. Hadži, D. Kocjan, V. Rutar, Org. Magn. Reson. 15 (1981) 280–284.
[62] G.D.G. Santonoceta, C. Sgarlata, Mol. Basel Switz. 28 (2023) 5581.